

# Time-Domain Based Embeddings for Spoofed Audio Representation

Matan Karo<sup>1</sup>, Arie Yeredor<sup>1</sup>, Itshak Lapidot<sup>2,3</sup>

<sup>1</sup>Tel Aviv University (TAU), School of Electrical Engineering, Israel

<sup>2</sup>Afeka Tel Aviv Academic College of Engineering, ACLP, Israel

<sup>3</sup>Avignon University, LIA, France

matankaro@mail.tau.ac.il, itshakl@afeka.ac.il, arie@eng.tau.ac.il

## Abstract

Anti-spoofing is the task of speech authentication. That is, identifying genuine human speech compared to spoofed speech. The main focus of this paper is to suggest new representations for genuine and spoofed speech, based on the probability mass function (PMF) estimation of the audio waveforms' amplitude.

We introduce a new feature extraction method for speech audio signals: unlike traditional methods, our method is based on direct processing of time-domain audio samples. The PMF is utilized by designing a feature extractor based on different PMF distances and similarity measures. As an additional step, we used filter-bank preprocessing, which significantly affects the discriminative characteristics of the features and facilitates convenient visualization of possible clustering of spoofing attacks. Furthermore, we use diffusion maps to reveal the underlying manifold on which the data lies.

The suggested embeddings allow the use of simple linear separators to achieve decent performance. In addition, we present a convenient way to visualize the data, which helps to assess the efficiency of different spoofing techniques.

The experimental results show the potential of using multi-channel PMF based features for the anti-spoofing task, in addition to the benefits of using diffusion maps both as an analysis tool and as an embedding tool.

**Index Terms:** anti-spoofing, speech embedding, speech probability mass function, diffusion maps

## 1. Introduction

Biometrics technologies have a major role in personal identification and authentication, voice-based systems in particular [1]. The purpose of an *Automatic Speaker Verification (ASV)* system is to validate the speaker's identity by analyzing an audio sample of his/her voice [2, 3]. ASV systems allow the user to authenticate its identity in a natural, non-invasive manner. As the use of ASV systems is becoming more popular, the interest in bypassing and exploiting them increases accordingly. Therefore, the issue of preventing attackers from exploiting such systems is necessary.

The counter task of speech spoofing, hence detecting the fraud, is called Anti-Spoofing, and it has been studied vastly as described, e.g., in selected surveys [4, 5]. Due to the importance of finding countermeasures, a series of anti-spoofing challenges has been published [6]. Numerous of studies have been made using the challenges databases, and comparisons between different methods can be found in [7, 8, 9]. Our work has been done primarily on the ASVspoof 2019 [10] *Logical Access (LA)* database.

Most speech features for anti-spoofing are based on frequency-domain analysis. There is almost no research directly addressing time-domain based features as spoofing coun-

termeasures. However, the time-domain representation contains information which is utilized for various tasks [11]. Previous work [12, 13] has shown that the *Probability Mass Function (PMF)* of genuine speech samples differs from the PMF of spoofed speech samples. Motivated by those results, our goal is to further expand such PMF-based methods by exploring the use of channel-based time-domain features. For exploring spoofed speech from a time-domain perspective, we propose a new feature extraction approach, which relies on estimating the samples' joint or marginal PMFs with the addition of filter-bank pre-processing.

In previous work, the probability mass function, which is equivalent to the normalized histogram of the audio samples' amplitude, was calculated across each set of the database as a whole. To get a better understanding of the separative characteristics of the speech PMF for the classification task, we have utilized the PMF in a different way, using it in the feature extraction process. First, gender-based labels have been added to the audio files under the assumption that the speaker's gender influences speech distribution [14]. Due to the pre-known target's gender in the ASV task, gender separation is a valid assumption. The effect of gender separation is discussed in Section 4.

The feature extractor included two global speakers models, genuine and spoofed, which were calculated as the PMF across the training set. Then, similarity measures (such as distance metrics) from each model were calculated for producing a single feature, corresponding to a specific measure. This process is given in further details in Section 2.

Frequently used features for the anti-spoofing are cepstral features [15], such as *Mel Frequency Cepstral Coefficients (MFCC)*, *Linear Cepstral Coefficients (LFCC)* and *Constant-Q Cepstral Coefficients (CQCC)* [16, 17]. Inspired by the feature extraction process of spectral coefficients, different filter-banks were applied to the audio samples. Each filter output created an output channel, for which the PMF distances from each global speaker model were calculated. The motivation was to identify dominant channels for the anti-spoofing task.

The main research objective was to gain new insights about genuine and spoofed speech and prominent differences between these two in the respective samples' PMFs. Due to the difficulty to distinguish between them, we have looked for new ways to embed the relations between genuine and spoofed speech, and between different attack methods. Therefore, this work's main focus is on feature representation other than optimizing a state-of-the-art classification scheme. For that purpose, we have used a manifold learning technique known as *Diffusion Maps (DM)* [18], for both visualization and features embedding. The use of DM revealed the discriminative quantities of the PMF method and provided new insights about the effectiveness of different attacks. A simple *Logistic Regression (LR)* was used for classification.

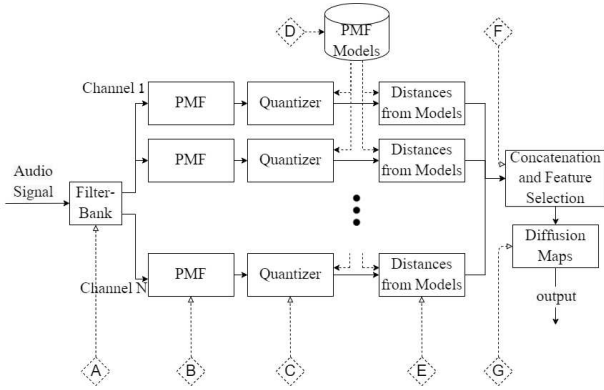


Figure 1: Features extraction scheme.

## 2. PMF-based Feature Extraction

This section describes the feature extraction process, or in other words, the embedding of human and spoofed speech utterances into a new representation. The core idea is that spoofed speech affects the amplitude's distribution in a way that will cause a distinguishable difference between human and spoofed speech. In both [12] and [13] PMFs of different datasets were calculated, showing differences between human and spoofed distributions. In this work, we have utilized the PMFs as a part of a feature extraction scheme whose illustration is given in Figure 1.

### 2.1. Filter-Banks

The design process of filter-bank in speech processing is frequently influenced by a biological or psychoacoustic model of the human hearing system/perception. Due to the use of such filters in anti-spoofing solutions, we chose to include them in our scheme, but with some integration modifications. To begin with, our PMF-based approach is meant to examine the samples in the time-domain instead of the frequency-domain, as is normally the case with filter-banks. Therefore, we applied the filtering process directly on the audio samples.

We chose to focus on two filter-banks types: Mel filter-bank (used in MFCC [19]) and Gammatone filter-bank (used in *Gammatone Cepstral Coefficients (GTCC)* [20]):

- **Mel Filter-Bank:** a set of triangular, variable bandwidths filters, spaced linearly on mel scale. The design simulates the non-linear frequency-sensitivity of the human hearing system - its resolution degrades as the frequency increases.
- **Gammatone Filter-Bank:** a set of gammatone filters, equally spaced on the ERB scale [21]. Gammatone filter banks were designed to model the human auditory system. Inspired by the cochlea structure, a gammatone filter-bank simulates its action by transforming complex sounds into a multichannel activity pattern, in a similar manner to the pattern observed in the auditory nerve.

Although the use of gammatone filter-banks not as common as the use of mel and linear filter-banks in traditional anti-spoofing solutions, gammatone based features have proven themselves both in speech recognition [22] and in anti-spoofing tasks [20, 23].

In this paper we will focus on the Gammatone filter-bank, which showed superior separative capabilities compared to the

Mel filter-bank. Furthermore, we have also used an inverted version of the Gammatone filter-bank, known as Inverse Gammatone filter-bank, which enabled to separate specific spoofing methods.

### 2.2. Probability Mass Function

The probability mass function (PMF) is a function which represents the probabilities of a discrete random variable to attain each of its possible values.. In our context, we will refer to the PMF as the normalized histogram of a discrete set of attainable values. Analog audio waveform representation is continuous, meaning its statistical representation should be done by using a continuous function such as *Probability Density Function (PDF)*. However, in this work's framework the audio samples are digital, hence quantized to a finite set of values. Therefore, the PMF is used and approximates the PDF of the real analog audio. This approximation depends on the bin width  $\Delta x$ , which is the width of each bin in the histogram. The *PMF* of bin  $x_0$  can be approximated by:

$$PMF(x = x_0) \approx \int_{x_0 - \frac{\Delta x}{2}}^{x_0 + \frac{\Delta x}{2}} PDF(x) dx \quad (1)$$

For waveform samples which are sampled using  $b$  bits per sample, there are  $2^b$  possible discrete values. For both ASVspoof 2015 and ASVspoof 2019 the LA audio files were sampled with 16 bits per sample and normalized to  $[-1, 1]$ , which dictates explicitly the histogram bins for the direct PMF calculation. The PMF calculation for filtered audio was done after inspecting the dynamic range of the output channels of the training set. After the inspection we chose to keep the bins the same and to clip exceeding values.

### 2.3. Similarity Measures

Inspired by the *Gaussian Mixture Model Universal Background Model (GMM-UBM)* [24] approach, which uses a global speaker model for the feature embedding process, we have also taken a global model-based approach. The PMFs calculated in [13] are utilized to represent a global human or spoofed speaker model. Models for human and spoofed speech have been constructed by calculating the PMF across corresponding audio files in the training set. Then, each audio file can be represented by a similarity measure to each model. To this end, a PMF similarity measure (such as distance metric), should be defined [25].

In [12] and [13], *Kullback-Leibler Divergence (KLD)* [26] was discussed as an evaluation metric for the similarity between PMFs. In our work, the use of KLD as a similarity measure was expended to using several similarity measures: quadratic Chi distance [27], normalized cross correlation [28], Hellinger distance [29], histogram intersection [30], Jensen-Shannon [31], Symmetrized Kullback-Leibler and Kullback-Leibler Divergence [26], and modified Kolmogorov-Smirnov [32].

### 2.4. Features Concatenation and Selection

Feature construction is the process of generating a single feature vector out of the extracted features. In our case, each extracted feature expresses the similarity of an input PMF to a model PMF under a certain measure for a specific channel. We have tested several concatenation schemes, some isolate each channel and distance combination, some concatenating groups of features and some more sophisticated methods which involved

pre processing before the concatenation. These schemes are described and compared in Section 4.

### 3. Diffusion Maps

Diffusion maps (DM) is a part of nonlinear dimensionality reduction methods called manifold learning, which is often also used for feature extraction. The main underlying assumption in such methods is that the high-dimensional sampled data lies on some low-dimension manifold in the high-dimensional ambient space. By utilizing the manifold structure, a reduced representation can be found, while preserving the local relations between the data samples. Diffusion maps technique has been used successfully in machine learning and data mining applications, including speech processing tasks [33, 34].

DM have an advantage over several other methods, such as the popular t-distributed stochastic neighbor embedding (t-sne) [35], due to its ability to conveniently expand its embedding to new samples. The out of sample extension ability is important in our case, due to the requirement to evaluate new data which may contain both previously observed and previously unobserved attacks.

Diffusion maps can be defined by three steps: connectivity, diffusion distance and diffusion maps embedding [36].

#### 3.1. Connectivity

Let  $\mathbf{X} = \{x_1, \dots, x_N\} \in \mathbb{R}^d$  be a  $d$ -dimensional set of  $N$  data-points.

The one-step transition probability from node  $x_i$  to  $x_j$  can be expressed by normalizing a kernel function asymmetrically by the nodes' degree:

$$p(x_i, x_j) = \frac{k_\epsilon(x_i, x_j)}{\deg(x_i)} \quad (2)$$

where  $k_\epsilon(x_i, x_j)$  is a kernel function, usually chosen as a Gaussian kernel with a width controlled by  $\epsilon$ , and  $\deg(x) = \sum_{y \in \mathbf{X}} k_\epsilon(x, y)$ . The elements of the transition matrix  $\mathbf{P}$  are given by Equation 2, and its bi-orthogonal right and left eigenvectors are denoted as  $\psi_k$  and  $\phi_k$ , with a sequence of eigenvalues:  $|\lambda_0| = 1 \geq |\lambda_1| \geq \dots \geq |\lambda_{d-1}|$ .

#### 3.2. Diffusion Distance

The diffusion distance measures the similarity of two points in the observation space, which reflects the intrinsic geometry of the underlying manifold. The diffusion distance at time  $t$  is calculated using the connectivity, e.g. the total transition probability of all connecting paths, which describes the  $t$ -step evolution of the probability distribution in a Markov chain. The diffusion distance can be expressed in terms of the eigenvectors of  $\mathbf{P}$ :

$$D_t(x_i, x_j)^2 = \sum_{k=1}^{d-1} \lambda_k^{2t} (\psi_k(x_i) - \psi_k(x_j))^2 \quad (3)$$

where  $\psi_0 = \mathbf{1}$  is excluded from the summation.

#### 3.3. Diffusion Maps Embedding

The dimensionality reduction is achieved by approximating the diffusion distance using a lower number of summation arguments. This is possible due to spectrum decay, which enables to approximate Equation 3 with a sufficient accuracy only by

using the  $K \ll d - 1$  first non constants eigenvectors:

$$D_t(x_i, x_j)^2 \approx \sum_{k=1}^K \lambda_k^{2t} (\psi_k(x_i) - \psi_k(x_j))^2 \quad (4)$$

Based on Equation 4, we can define the following mapping:

$$\Psi_t : x \rightarrow (\lambda_1^t \psi_1(x), \lambda_2^t \psi_2(x), \dots, \lambda_K^t \psi_K(x))^T \quad (5)$$

The mapping  $\Psi_t$  embeds the dataset  $\mathbf{X}$  into the Euclidean space  $\mathbb{R}^K$ , hence reducing the original dimension  $d$  to  $K$ . The diffusion distance between two points in the original dataset is equivalent to the Euclidean distance between their embeddings [37]:

$$D_t(x_i, x_j)^2 \approx \|\Psi_t(x_i) - \Psi_t(x_j)\|^2 \quad (6)$$

#### 3.4. Out of Sample Extension

For large datasets the diffusion map embedding becomes impractical, as a result of oversized kernel matrix. A solution for this is to construct the embedding scheme using a subset of the complete dataset, and then apply the diffusion map to the entire dataset using an *Out Of Sample (OOS)* extension method. In our framework we have chosen to use the most popular method, known as the Nyström's extension method, due to its simplicity and well proven performance [38]. Given a new point  $x' \notin \mathbf{X}$  the eigenvector  $\psi_k$  is extended to this point as follows:

$$\hat{\psi}_k(x') = \frac{1}{\lambda_k} \sum_{y \in \mathbf{X}} p(x', y) \psi_k(y), k = 1, \dots, K \quad (7)$$

## 4. Experiments

As mentioned before, the main goal of our work was to gain new insights by inspecting spoofed and genuine speech in time-domain perspective. Therefore, we did not try to optimize a classifier for the embeddings, but rather focused on the embeddings representation. However, we have used a simple logistic regression classifier to quantify and compare different embeddings in terms of error rates and *Equal Error Rate (EER)*.

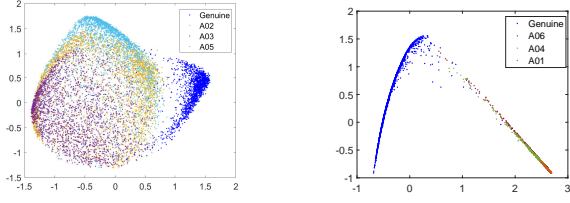
In the following experiments we have used Gammatone and Inverse Gammatone filter-banks, each with 10 channels spanned from 0kHz to 8kHz. Unless mentioned otherwise, the experiments were conducted on the ASVspoof2019 database. The global speakers' PMFs were calculated per gender unless specified otherwise. In any case of DM use, it was trained using 7000 samples from the training set, 1000 from each spoofing attack and 1000 genuine, and  $t$  was set to 1.

We have created a single feature vector by concatenation in the following manner: All eight similarity measures under a given channel were concatenated by the order described in Section 2, followed by additional concatenation of the length-8 blocks by an ascending channel order. This process repeated itself twice, for both genuine and spoofed models, and the resulting features vectors were subtracted from each other for creating a single feature vector.

Denote  $d_l^{(i)}(p_1, p_2)$  as the  $l^{th}$  similarity measure between two PMFs,  $p_1$  and  $p_2$ , under the  $i^{th}$  channel of an arbitrary filter-bank. Given the PMF of an input file  $p_{input}$ , the feature vector based on  $I$  channels can be described as:

$$\mathbf{f} = (s_1^{(1)}, s_2^{(1)}, \dots, s_8^{(1)}, s_1^{(2)}, \dots, s_8^{(I)}) \quad (8)$$

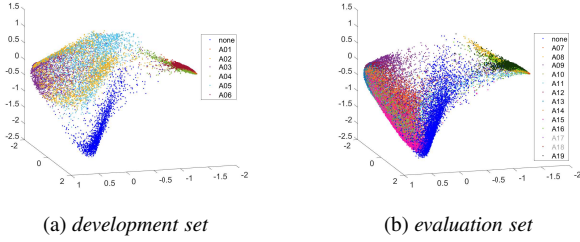
where  $s_l^{(i)} = d_l^{(i)}(p_{input}, p_{spoofed}) - d_l^{(i)}(p_{input}, p_{genuine})$  and  $p_{spoofed}, p_{genuine}$  are the PMFs models mentioned in Section 2.2. The feature vector introduced in Equation 8 is referred



(a) Gammatone with 10 channels

(b) Inverse Gammatone with 10 channels

Figure 2: Gammatone vs. Inverted Gammatone DM embedding for all channels and metrics. The embeddings are done on all female samples of development set.



(a) development set

(b) evaluation set

Figure 3: DM embedding on all channels and distance metrics of Gammatone and Inverse Gammatone with 10 channels. The embeddings in this figure were made on all female samples.

as "full filter-bank feature vector". The "full feature vector" is created by concatenation of two "full filter-bank feature vectors", corresponding to the Gammatone and Inverse Gammatone filter-banks. Other features representations may be created by taking only partial channels or distance metrics. This is done by omitting the corresponding features from the "full feature vector".

#### 4.1. Full Feature Embeddings

In this experiment, we show how the "full filter-bank feature vector" is embedded using a DM, and how this embedding clusters different spoofing attacks. It is interesting to see in Figure 2 how each filter-bank acts differently on the attacks. The Gammatone manages to separate well A02, A03 and A05 (all share the same waveform generator) while the Inverse Gammatone separates A01, A04 and A06. Figure 3 demonstrates how the concatenation of the filter-banks using the DM enables full separation of all training attacks.

#### 4.2. Reduced Feature Embeddings

Not all components of channels and metrics contribute to the separative characteristics of the "full feature vector". Removing some of them affects the geometric layout of the embedded samples, and in some cases increases the linear separability of the clusters. An example for such a configuration is keeping only the 5 low channels from each filter-bank, and selecting the similarity measures as follow: measures 1-5 for Gammatone and measures 1-6 excluding 4 for the Inverse Gammatone (the numbers correspond to the order by which the similarity measures were presented in Section 2). We will refer to this configuration as the "reduced configuration". An illustration of the embeddings under "reduced configuration" is given in Fig-

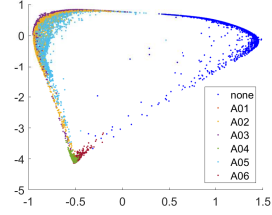


Figure 4: DM embeddings of "reduced configuration" on female development set.

Table 1: Error rate according to EER threshold under "reduced configuration". The error rates are given in [female] / [male] format. The overall EER is the same as the "None"

Attack	Error on Train [%]	Error on Dev [%]	Attack	Error on Eval [%]
None	0.33 / 5.11	0.12 / 2.07	None	12.99 / 12.09
A01	0.00 / 0.00	0.00 / 0.00	A07	0.00 / 0.00
A02	0.00 / 0.06	0.00 / 0.00	A08	0.00 / 0.00
A03	0.00 / 0.12	0.08 / 0.00	A09	0.00 / 1.78
A04	0.00 / 0.00	0.00 / 0.00	A10	2.76 / 2.05
A05	0.58 / 30.48	0.48 / 12.58	A11	1.88 / 2.97
A06	1.61 / 0.00	0.16 / 0.00	A12	0.00 / 0.13
			A13	0.00 / 0.06
			A14	0.61 / 1.25
			A15	11.46 / 4.16
			A16	0.00 / 0.00
			A17	74.01 / 67.72
			A18	78.22 / 77.44
			A19	0.00 / 0.00

ure 4 and its error rate table using a LR is given in Table 1. The front-ends are the 4 dimensional DM embeddings, and the threshold of the LR is set according to EER of each set. The table shows how A05 acts differently according to the speakers' gender and that A17 and A18 (both are voice conversion attack) are the hardest attacks across all seen and unseen attacks.

In Table 2 we present the total EER by gender across two databases, ASVspooft2015 and ASVspooft2019, using the "reduced configuration". We have used 4 DM features for male samples, and 5 for female (the number of features was chosen according the development sets of both databases). It is obvious that the advanced spoofing techniques presented in ASVspooft2019 make it harder to find a generalizing spoofing countermeasures.

Table 2: EER comparison on "reduced configuration" representation across different LA databases. The results were calculated using logistic regression and are given by set: train / dev / eval.

Database	Female EER [%]	Male EER [%]
ASVspooft2015	0.57 / 0.35 / 1.83	1.40 / 2.80 / 2.27
ASVspooft2019	0.32 / 0.12 / 12.99	5.11 / 2.07 / 12.09

## 5. Conclusions

In this work we have shown a new time-domain PMF-based perspective to represent genuine and spoofed audio. We have utilized diffusion maps for both visualization and feature reduction. The use of the DM has helped us to design a feature extraction scheme and to better understand the role of each feature. We showed that under our representation the separative information lies mostly in low to mid filter-bank channels and that some spoofing attacks acts differently on different genders.

In addition, the use of DM embedding allowed us to use a very simple linear classifier for gaining decent error rates.

## 6. References

- [1] S. Singh, "The role of speech technology in biometrics, forensics and man-machine interface," *International Journal of Electrical and Computer Engineering (IJECE)*, vol. 9, no. 1, p. 281, Feb. 2019.
- [2] T. Kinnunen and H. Li, "An overview of text-independent speaker recognition: From features to supervectors," *Speech Communication*, vol. 52, no. 1, pp. 12–40, Jan. 2010.
- [3] J. H. Hansen and T. Hasan, "Speaker Recognition by Machines and Humans: A tutorial review," *IEEE Signal Processing Magazine*, vol. 32, no. 6, pp. 74–99, Nov. 2015.
- [4] Z. Wu, N. Evans, T. Kinnunen, J. Yamagishi, F. Alegre, and H. Li, "Spoofing and countermeasures for speaker verification: A survey," *Speech Communication*, vol. 66, pp. 130–153, Feb. 2015.
- [5] Z. Wu, P. L. De Leon, C. Demiroglu, A. Khodabakhsh, S. King, Z.-H. Ling, D. Saito, B. Stewart, T. Toda, M. Wester, and J. Yamagishi, "Anti-Spoofing for Text-Independent Speaker Verification: An Initial Database, Comparison of Countermeasures, and Human Performance," *IEEE/ACM Transactions on Audio, Speech, and Language Processing*, vol. 24, no. 4, pp. 768–783, Apr. 2016.
- [6] "ASVspoof," <https://www.asvspoof.org/>.
- [7] M. R. Kamble, H. B. Sailor, H. A. Patil, and H. Li, "Advances in anti-spoofing: From the perspective of ASVspoof challenges," *APSIPA Transactions on Signal and Information Processing*, vol. 9, p. e2, 2020.
- [8] A. Nautsch, X. Wang, N. Evans, T. H. Kinnunen, V. Vestman, M. Todisco, H. Delgado, M. Sahidullah, J. Yamagishi, and K. A. Lee, "ASVspoof 2019: Spoofing Countermeasures for the Detection of Synthesized, Converted and Replayed Speech," *IEEE Transactions on Biometrics, Behavior, and Identity Science*, vol. 3, no. 2, pp. 252–265, Apr. 2021.
- [9] M. Sahidullah, H. Delgado, M. Todisco, T. Kinnunen, N. Evans, J. Yamagishi, and K.-A. Lee, "Introduction to Voice Presentation Attack Detection and Recent Advances," in *Handbook of Biometric Anti-Spoofing*, S. Marcel, M. S. Nixon, J. Fierrez, and N. Evans, Eds. Cham: Springer International Publishing, 2019, pp. 321–361.
- [10] M. Todisco, X. Wang, V. Vestman, M. Sahidullah, H. Delgado, A. Nautsch, J. Yamagishi, N. Evans, T. H. Kinnunen, and K. A. Lee, "ASVspoof 2019: Future Horizons in Spoofed and Fake Audio Detection," in *Interspeech 2019*. ISCA, Sep. 2019, pp. 1008–1012.
- [11] J. Ruzs, R. Cmejla, H. Ruzickova, and E. Ruzicka, "Quantitative acoustic measurements for characterization of speech and voice disorders in early untreated Parkinson's disease," *The Journal of the Acoustical Society of America*, vol. 129, no. 1, pp. 350–367, Jan. 2011.
- [12] I. Lapidot, H. Delgado, M. Todisco, N. Evans, and J.-F. Bonastre, "Speech Database and Protocol Validation Using Waveform Entropy," in *Interspeech 2018*. ISCA, Sep. 2018, pp. 2773–2777.
- [13] I. Lapidot and J.-F. Bonastre, "Effects of Waveform PMF on Anti-Spoofing Detection," in *Interspeech 2019*. ISCA, Sep. 2019, pp. 2853–2857.
- [14] J. Jensen, I. Batina, R. Hendriks, and H. Richard, "A STUDY OF THE DISTRIBUTION OF TIME-DOMAIN SPEECH SAMPLES AND DISCRETE FOURIER COEFFICIENTS," Jan. 2005.
- [15] M. Sahidullah, T. Kinnunen, and C. Hanilçi, "A comparison of features for synthetic speech detection," in *Interspeech 2015*. ISCA, 2015, pp. 2087–2091.
- [16] X. Zhou, D. Garcia-Romero, R. Duraiswami, C. Espy-Wilson, and S. Shamma, "Linear versus mel frequency cepstral coefficients for speaker recognition," in *2011 IEEE Workshop on Automatic Speech Recognition Understanding*, Dec. 2011, pp. 559–564.
- [17] M. Todisco, H. Delgado, and N. Evans, "A New Feature for Automatic Speaker Verification Anti-Spoofing: Constant Q Cepstral Coefficients," in *The Speaker and Language Recognition Workshop (Odyssey 2016)*. ISCA, Jun. 2016, pp. 283–290.
- [18] R. R. Coifman and S. Lafon, "Diffusion maps," *Applied and Computational Harmonic Analysis*, vol. 21, no. 1, pp. 5–30, Jul. 2006.
- [19] S. S. Tirumala, S. R. Shahamiri, A. S. Garhwal, and R. Wang, "Speaker identification features extraction methods: A systematic review," *Expert Systems with Applications*, vol. 90, pp. 250–271, Dec. 2017.
- [20] X. Valero and F. Alias, "Gammatone Cepstral Coefficients: Biologically Inspired Features for Non-Speech Audio Classification," *IEEE Transactions on Multimedia*, vol. 14, no. 6, pp. 1684–1689, Dec. 2012.
- [21] M. Slaney, "An efficient implementation of the Patterson-Holdsworth auditory filter bank," *Apple Computer, Perception Group, Tech. Rep.*, vol. 35, no. 8, 1993.
- [22] C. Kim and R. M. Stern, "Power-Normalized Cepstral Coefficients (PNCC) for Robust Speech Recognition," *IEEE/ACM Transactions on Audio, Speech, and Language Processing*, vol. 24, no. 7, pp. 1315–1329, Jul. 2016.
- [23] Z. Oo, L. Wang, K. Phapatanaburi, M. Liu, S. Nakagawa, M. Iwahashi, and J. Dang, "Replay attack detection with auditory filter-based relative phase features," *EURASIP Journal on Audio, Speech, and Music Processing*, vol. 2019, no. 1, p. 8, Jun. 2019.
- [24] D. A. Reynolds, T. F. Quatieri, and R. B. Dunn, "Speaker Verification Using Adapted Gaussian Mixture Models," *Digital Signal Processing*, vol. 10, no. 1, pp. 19–41, Jan. 2000.
- [25] S.-H. Cha and S. N. Srihari, "On measuring the distance between histograms," *Pattern Recognition*, vol. 35, no. 6, pp. 1355–1370, Jun. 2002.
- [26] S. Kullback and R. A. Leibler, "On Information and Sufficiency," *The Annals of Mathematical Statistics*, vol. 22, no. 1, pp. 79–86, Mar. 1951.
- [27] O. Pele and M. Werman, "The Quadratic-Chi Histogram Distance Family," in *Computer Vision – ECCV 2010*, ser. Lecture Notes in Computer Science, K. Daniilidis, P. Maragos, and N. Paragios, Eds. Berlin, Heidelberg: Springer, 2010, pp. 749–762.
- [28] K. Briechele and U. D. Hanebeck, "Template matching using fast normalized cross correlation," in *Aerospace/Defense Sensing, Simulation, and Controls*, D. P. Casasent and T.-H. Chao, Eds., Orlando, FL, Mar. 2001, pp. 95–102.
- [29] E. Hellinger, "Neue Begründung der Theorie quadratischer Formen von unendlichvielen Veränderlichen," *Journal für die reine und angewandte Mathematik*, vol. 1909, no. 136, pp. 210–271, Jul. 1909.
- [30] M. J. Swain and D. H. Ballard, "Color indexing," *International Journal of Computer Vision*, vol. 7, no. 1, pp. 11–32, Nov. 1991.
- [31] J. Lin, "Divergence measures based on the Shannon entropy," *IEEE Transactions on Information Theory*, vol. 37, no. 1, pp. 145–151, Jan. 1991.
- [32] "Tech. Report: Modified Kolmogorov-Smirnov test," 2020.
- [33] R. Talmon, I. Cohen, and S. Gannot, "Clustering and suppression of transient noise in speech signals using diffusion maps," in *2011 IEEE International Conference on Acoustics, Speech and Signal Processing (ICASSP)*, May 2011, pp. 5084–5087.
- [34] —, "Single-channel transient interference suppression with diffusion maps," *IEEE Transactions on Audio, Speech, and Language Processing*, vol. 21, no. 1, pp. 132–144, Jan. 2013.
- [35] L. Van der Maaten and G. Hinton, "Visualizing data using t-SNE," *Journal of machine learning research*, vol. 9, no. 11, 2008.
- [36] J. Porte, B. Herbst, W. Hereman, and S. van der Walt, "An Introduction to Diffusion Maps," Nov. 2008.
- [37] B. Nadler, S. Lafon, R. R. Coifman, and I. G. Kevrekidis, "Diffusion Maps, Spectral Clustering and Eigenfunctions of Fokker-Planck operators," *arXiv:math/0506090*, Jun. 2005.

- [38] M.-A. Belabbas and P. J. Wolfe, "Spectral methods in machine learning and new strategies for very large datasets," *Proceedings of the National Academy of Sciences*, vol. 106, no. 2, pp. 369–374, Jan. 2009.